Sensors & Diagnostics

PAPER

View Article Online
View Journal | View Issue

Cite this: *Sens. Diagn.*, 2023, **2**, 1597

Rapid detection of *Candida albicans* in urine by an Electrochemical Impedance Spectroscopy (EIS)-based biosensor†

Tina D'Aponte, [a] Maria De Luca, [a] Nikola Sakač, [b] Martina Schibeci, [c] Angela Arciello, [c] Emanuela Roscetto, [d] Maria Rosaria Catania, [d] Vincenzo Iannotti, [ae] Raffaele Velotta [a] and Bartolomeo Della Ventura *[a]

Candida albicans is a fungal organism commonly found in the human body, including the genitourinary tract. Overgrowth of this yeast can lead to candiduria, the abnormal presence of *C. albicans* in urine. The detection of candiduria relies on various methods that offer sensitivity and specificity for accurate diagnosis, but none of them is rapid and cost-effective. Biosensors may offer an answer; in particular, impedance-based biosensors have shown promise in addressing the detection of *C. albicans* since they offer high sensitivity, simplicity of fabrication, excellent selectivity, real-time detection, and cost-effectiveness. However, variations in the working surface of commercial screen-printed electrodes as well as manual functionalization can impact robustness and reproducibility. In this paper, we describe significant advances that we introduced to perform electrochemical impedance spectroscopy for biosensing purposes. Specifically, we designed a microfluidic cell for standardizing the electrode functionalization and target detection, ensuring sensor reproducibility and robustness. By optimizing several parameters like the flow rate and the density of antibodies on the electrode surface, we could achieve a limit of detection of 10 CFU mL^{-1} in urine with a measurement that lasted for less than 90 minutes. The modularity of the device and the measurement procedure makes the described biosensor extendable for conducting high-throughput analyses.

Received 3rd August 2023,
Accepted 3rd October 2023

DOI: 10.1039/d3sd00209h

rsc.li/sensors

Introduction

Candida albicans is a fungal organism that commonly inhabits the human body, including the genitourinary tract.[1,2] However, when this yeast overgrows, it can lead to a condition called candiduria, which involves the presence of *C. albicans* in urine. Candiduria is a significant issue that affects individuals of all ages and genders,[3] particularly those with weakened immune systems or specific predisposing factors.[4] Understanding the causes, symptoms, diagnosis, and treatment of candiduria is crucial for the effective management and prevention of complications.

The gold standard method for diagnosing candiduria is urine culture. It involves inoculating urine samples onto appropriate culture media, such as Sabouraud dextrose agar or chromogenic agar, which selectively promote the growth of *Candida* species.[5,6] Colonies are then identified through morphological characteristics, biochemical tests, or automated systems.[7] This method provides both qualitative and quantitative information, but it is time-consuming since approximately 48 hours are required to obtain a response.

Polymerase chain reaction (PCR)[8,9] and other molecular techniques have emerged as valuable tools for detecting *Candida* DNA in urine samples. These methods target specific *Candida* genes or regions and offer high sensitivity and specificity. PCR can differentiate between various *Candida* species and even detect low fungal loads. However, it is worth evidencing that PCR assays for *Candida* detection in urine typically do not provide quantitative information regarding the fungal load. This limitation may hinder the ability to determine the severity of infection or monitor treatment responses accurately.[10]

Enzyme-linked immunosorbent assays (ELISAs) are already utilized for *Candida* detection and demonstrate a good limit of detection (LOD). However, they are still associated with relatively long waiting times for obtaining results.[11]

[a] *Department of Physics "Ettore Pancini", University of Naples "Federico II", 80126 Naples, Italy. E-mail: bartolomeo.dellaventura@unina.it*
[b] *Faculty of Geotechnical Engineering, University of Zagreb, 42000 Varaždin, Croatia*
[c] *Department of Chemical Sciences, University of Naples "Federico II", 80126 Naples, Italy*
[d] *Department of Molecular Medicine and Medical Biotechnology, University of Naples "Federico II", 80131 Naples, Italy*
[e] *CNR – SPIN (Institute for Superconductors, Oxides and other Innovative Materials and Devices), Piazzale V. Tecchio 80, 80125 Naples, Italy*

† Electronic supplementary information (ESI) available. See DOI: https://doi.org/10.1039/d3sd00209h

In the last year, Matrix-Assisted Laser Desorption/Ionization Time-of-Flight Mass Spectrometry MALDI-TOF MS has revolutionized microbial identification, including *Candida* species, since this technique analyses the protein profiles of microbial colonies and allows for rapid and accurate identification, even at the species level. Moreover, it can be applied to colonies obtained from urine culture. However, each of these methods has its own set of advantages and limitations, including factors like availability, cost, laboratory expertise, and the clinical context in which the test is being performed.[12,13]

Biosensors with enhanced sensitivity, selectivity, and ease-of-use would be crucial for improving the diagnosis and management of candiduria. In fact, a variety of biosensors have been proposed for the detection of *Candida*, offering different advantages and performance characteristics. Optical biosensing techniques,[14] such as surface plasmon resonance and fluorescence-based assays,[15,16] utilize the interaction of light with *Candida*-specific biomarkers for detection. Although they provide high sensitivity and real-time monitoring capabilities,[17] these biosensors often require complex instrumentation, labelling processes, and expert personnel.

Electrochemical biosensors are emerging as a powerful tool for detecting pathogens in biological fluids such as blood, sweat, saliva, tears, and urine.[18,19] This technology is also suitable for portable and wearable devices, allowing continuous monitoring and enabling early management in diagnostics.[20,21] In particular, electrochemical biosensors offer an alternative approach for detecting *Candida* cells by leveraging their electrochemical properties.[22] For instance, amperometric[23] and potentiometric[20] biosensors utilize the measurement of current or potential changes, respectively, upon *Candida* interaction. These biosensors demonstrate good sensitivity, simplicity, and cost-effectiveness, but they may suffer from limited selectivity due to non-specific interactions.

Impedance-based biosensors,[24,25] which measure changes in electrical impedance resulting from *Candida*-cell interactions,[26,27] have shown promise in addressing the limitations of previous biosensors. They provide high sensitivity, simplicity of fabrication, and excellent selectivity for *Candida* detection; in fact, sometimes they can even discriminate between different species of *Candida* with good sensitivity.[28,29] Further, impedance-based biosensors offer real-time and label-free detection, enabling rapid analysis of samples without additional reagents. In this scenario, they have the potential to improve early diagnosis and accuracy in detecting candiduria due to all their advantages, while overcoming the disadvantages of the currently most widely used techniques (such as time and cost).

The use of screen-printed electrodes (SPEs) makes them cost-effective and reliable. The increasingly widespread use of SPEs in recent years could lead to acceleration in the development of SPE-based electrochemical sensors in various fields, including health monitoring.[30] However, several limitations can arise, including robustness and reproducibility, due to variations in the working surface of each electrode, even if minimal, and the different conditions of manual drop-by-drop functionalization.[31,32]

In fact, electrochemical measurements are often conducted by incubating SPEs in various solutions. This serves two primary purposes: i) functionalizing the surface of the working electrode with antibodies, and ii) facilitating interaction with the analyte to be detected. The actual measurement is then performed in an electrolyte solution. However, this procedure leads to poor measurement reproducibility. The main issue arises because in addition to binding to the working electrode, both the antibodies and the analytes may also bind to the other two electrodes (auxiliary and counter electrodes). To address this challenge, we developed a microfluidic system that allows solutions to interact exclusively with the working electrode before SPEs are manually introduced into the electrochemical cell. It's worth noting that the use of microfluidics inherently reduces the operator dependence. With this approach, we have not only improved the performance of the biosensor but also minimized operator-related variability.

Experimental

Chemicals and materials

Potassium hexacyanoferrate(II) trihydrate ($K_4Fe(CN)_6{\cdot}3H_2O$), potassium hexacyanoferrate(III) ($K_3Fe(CN)_6$), bovine serum albumin (BSA) and sulphuric acid (H_2SO_4 98%) were purchased from Sigma-Aldrich (Milano, Italy). Phosphate buffered saline (PBS, 0.01 M, pH 7.4) was prepared by dissolving PBS tablets (from Gold Bio, St Louis, MO, USA) in Milli-Q water; each tablet prepares 100 mL of a 0.01 M PBS solution. Polyclonal antibodies (5.0 mg mL^{-1}) against *C. albicans* were purchased from Fitzgerald Industries. All water-based solutions were prepared in ultrapure water (24 MΩ cm) using a Milli-Q system.

Gold screen printed electrodes (AuSPEs) were purchased from BVT Technologies (Stražek, Czech Republic). They consist of a gold disk-shaped working electrode (d = 1 mm), a silver/silver chloride reference electrode and a gold counter electrode. These three electrodes were printed onto a corundum ceramic base measuring 0.7 × 2.5 cm^2. All potential values were referred to the silver/silver chloride reference electrode.

C. albicans in GYP

C. albicans ATCC® 10231 cells were cultured in glucose–yeast extract–peptone (GYP) medium (glucose 20 g L^{-1}; yeast extract 10 g L^{-1}; peptone 20 g L^{-1}) at 37 °C until exponential growth was reached. Afterwards, the optical density of the culture was measured, and the cells were diluted in 1/16 GYP medium at 2×10^6 CFU mL^{-1} before performing the analyses.

Bacterial strain *E. coli* ATCC 25922 was grown in Muller Hinton broth (MHB, Becton Dickinson Difco, Franklin Lakes, NJ, USA) and on tryptic soy agar (TSA; Oxoid Ltd., Hampshire, UK). In all the experiments, bacteria were inoculated and grown overnight in MHB at 37 °C. The next day, bacteria were

centrifuged and solubilized in 1× PBS at the desired cell densities (10^1–10^6 CFU mL^{-1}). By colony counting assays, it was verified that bacterial growth was negligible in 1× PBS with respect to MHB through a time interval of 3 hours at room temperature, whereas bacterial death was not observed.

C. albicans in urine

Waste aliquots of urine samples used for quality controls were processed on dipslides (Urotube – Liofilchem) containing three different culture media (CLED agar, MacConkey agar, Sabouraud dextrose agar) and incubated for 48 hours at 37 °C to verify the absence of bacterial and fungal growth. Sterile urine aliquots were used for subsequent studies. Suspensions of the reference strain ATCC 10231 *C. albicans* were prepared at different concentrations (10^n CFU mL^{-1} with n = 0, 1…7) in sterile urine aliquots. A control test was performed in sterile urine with null *C. albicans* concentration. The urine samples were real, anonymous urine samples, intended for disposal after being used as internal controls to test clinical biochemistry instrumentation. Before they were discarded, we used them for our experiments.

Electrochemical cell

Electrochemical Impedance Spectroscopy (EIS) and cyclic voltammetry (CV) measurements were carried out by dipping the electrode into a beaker containing 3 mL of redox probe solution [$Fe(CN)_6^{3-}$/$Fe(CN)_6^{4-}$ (1 : 1, 40 mM)] at room temperature. The potentiostat and impedance analyser was a PALMSENS (model PalmSens3, Utrecht, The Netherlands) controlled using a computer through the PSTRACE version 5.5 software (Fig. 1a).

EIS measurements were performed at frequencies that ranged from 0.5 Hz to 10 000 Hz at a formal potential of 0.16 V and using an amplitude perturbation of 10 mV.

The interaction of the *Candida* cells with the working electrode of the SPE was realized using a customized fluidic cell featuring an inlet that exclusively targets the working surface while keeping the auxiliary and reference electrodes isolated from the solutions. This cell is shown in Fig. 1b, in which the microfluidic cell is depicted in X-ray view, providing a clear visualization of the specific geometry utilized to selectively wet the working electrode without affecting the adjacent two electrodes.

In fact, microfluidics plays a crucial role in enhancing the capabilities of EIS and its integration with EIS offers several advantages for impedance-based biosensors. Firstly, microfluidic devices enable precise control and manipulation of fluid flow, allowing for a uniform distribution of samples and reagents across the sensing area. This uniformity ensures consistent and reliable measurements, minimizing variations that may arise from manual handling. Secondly, microfluidic channels can be designed to optimize the interaction between *Candida* cells and the electrode surface.

In this regard, by controlling the flow rate, cell concentration, and flowing time, the detection sensitivity can be optimized. The confined microscale environment also facilitates efficient mass transport, ensuring enhanced sensitivity and faster response times.

SPE cleaning procedure

The gold screen-printed electrodes were electrochemically cleaned using a 50 mM sulfuric acid (H_2SO_4).[33] The potential was cycled from −0.4 V to 1.4 V, with a scan rate of 0.1 V s^{-1}, until the cyclic voltammogram became stable (typically it took approximately 12 cycles). The electrode was then rinsed thoroughly with PBS and immersed in the electrolyte solution.

Fig. S1a† shows the CV scans obtained before and after the cleaning procedure. The CV signal is that obtained after six scans in the range −0.6 V to +0.6 V, with a scan rate of 0.1 V. The CV scan after cleaning shows an increase in current, indicating a cleaner surface. Moreover, this procedure allowed us to measure the redox potential of the $Fe(CN)_6^{3-}$/$Fe(CN)_6^{4-}$ solution, ultimately obtaining the formal potential of the redox couple for the subsequent EIS measurements. It is worth noticing that after cleaning, a reduction in

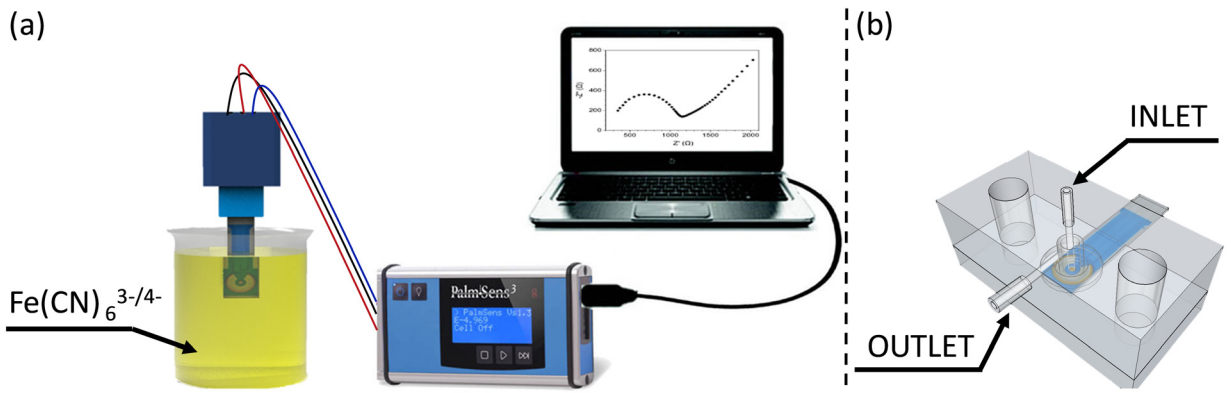

Fig. 1 (a) Scheme of the setup used for the electrochemical measurements: AuSPE was dipped in a beaker and connected to a potentiostat through a holder (dark blue) for the impedance measurements. (b) Microfluidic cell designed to deliver the solutions solely onto the gold electrode.

impedance is also observed (as illustrated in Fig. S1b†); in particular, a lower R_{CT} is revealing of a cleaner surface.

Electrode functionalization

The functionalization of the gold working electrode was accomplished using the Photochemical Immobilization Technique (PIT),[34,35] which allows for the covalent attachment of IgG antibodies specific to *C. albicans*. This technique ensures that the fragment antigen binding site (Fab) of the antibodies is adequately exposed to the solution. To achieve this, antibodies in a solution (25 μg mL^{-1}) were activated by UV-C light from a low-pressure mercury lamp, delivering approximately 0.3 W cm^{-2}. The irradiation lasted for 30 seconds, after which the solution was introduced into the microfluidic cell and flowed over the working electrode of the AuSPE for 15 minutes. This duration was chosen as a trade-off between the short time required by PIT (the produced thiol is effective for approximately 10 minutes)[34] and the extended time needed to conserve Abs (as a consumable material). Subsequently, a washing step with PBS was carried out to eliminate non-bonded Abs. The sequence of Abs irradiation, solution flow, and washing was repeated several times to optimize the surface coverage (see the section Results and discussion).

EIS data fitting

In EIS, the data from impedance measurement are usually represented by a Nyquist plot, in which each point represents the response of the electrochemical cell at different frequencies of input voltage (Fig. S2a†). The simplest equivalent circuit to model the behaviour of the cell is the Randles circuit (Fig. S2b†).[36] This circuit is composed of the resistance of the electrolyte solution (R_S), the double-layer capacitance (C_{DL}), the Warburg impedance (W) and the charge transfer resistance R_{CT}. R_S and W represent the bulk properties of the electrolyte solution and the diffusion features of the redox probe. These values are not influenced by modification on the electrode surface and are not modified by the antibodies–analyte interaction. In contrast, R_{CT} depends critically on the dielectric and insulating features at the electrode–electrolyte interface; thus, since it is very sensitive to electrode modifications, it was used as a biosensing parameter.

Frequently, the ideal capacitor C_{DL} is replaced by a constant phase element CPE (Fig. S2c†) to account for inhomogeneity and defect areas of the biological layer. This element can fit the imperfect behaviour of the double-layer capacitance due to the porosity or the roughness of the electrode area.

A version of the Randles circuit reported in Fig. S2c† was used to find R_{CT} from the Nyquist plots at the various target concentrations. To this aim, we relied on a tool from the PSTrace 5.5 software that used the Levenberg–Marquardt algorithm.

Results and discussion

Optimization of the functionalization procedure

The biosensor described in this paper has several parameters that need to be optimized. In particular, both the flow rate, which affects the streamline distribution and the velocity of the particles, and the degree of surface coverage are crucial for sensitivity. We started by measuring the kinetics of the surface coverage by (UV-activated) antibodies at different flow rates. The results are shown in Fig. 2(a)–(d), in which n stands for the number of times the sequence of steps – UV activation of Abs, flowing of Abs solution and washing (see the Electrode functionalization section) – was carried out. The surface blocking was realized by conveying a solution of BSA [50 μg mL^{-1}] to the cell for 15 minutes. As Fig. 2 shows, after each stage (n = 1, 4), while the impedance increased as a result of the presence of Abs on the surface, no significant change of impedance was produced by BSA. This means that for all the investigated flow rates, four functionalization stages – each including 15 minutes of UV-activated Abs flowing into the cell – were enough to fully cover the electrode surface.

As is evident from Fig. 2, even the bare SPEs show different behavior (Nyquist plot and R_{ct}) after the cleaning procedure – a feature that is unavoidable with typical commercial electrodes. To take into account the electrode variability, we normalized the change of the charge transfer resistance to its initial value $R_{ct\ bare}$

$$r_f = \frac{R_{ct\ abs} - R_{ct\ bare}}{R_{ct\ bare}} \quad (1)$$

In eqn (1), $R_{ct\ abs}$ is the value of R_{ct} measured after four functionalization stages. By using the ratio r_f, the influence

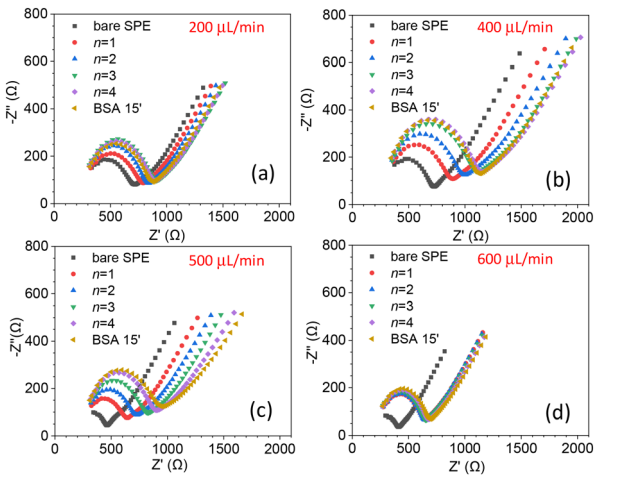

Fig. 2 EIS spectra obtained with different flow rates. The value n corresponds to the number of times the sequence of steps for the functionalization (UV activation of Abs, flowing of Abs solution and washing) was carried out. The EIS spectra were measured after the washing and the last step is the blocking realized with BSA that flowed for 15 minutes. From (a)–(d), we observe different behaviors at various flow speeds.

of the electrode characteristics and the background noise are minimized, allowing for a more accurate assessment of the surface changes. The analysis of the Nyquist plots with $n = 4$ shown in Fig. 2 is reported in Fig. S3,† which led us to choose a value of 450 μL min^{-1} for the flow rate.

As a further check of the binding kinetics of Abs to the surface, we fixed the flow rate at 450 μL min^{-1} and measured r_f after several functionalization stages. The results are reported in Fig. S4,† from which we deduced that $n = 4$ stages are sufficient to achieve saturation, *i.e.*, an electrode surface fully covered by Abs.

Since the degree of surface coverage by antibodies plays a crucial role in the charge transfer impedance, we wondered whether $n \geq 4$ (surface fully covered by Abs) led to an optimal response for EIS, or rather, a surface with a lower degree of coverage could give rise to a stronger variation of R_{ct}. The reason behind this question is that when the surface is fully covered, it may restrict the current variations resulting from target recognition, ultimately hampering the resistance change. To determine the optimal degree of surface coverage, we measured the change in R_{ct} induced by a relatively low concentration of *C. albicans* (10^2 CFU mL^{-1}) using electrodes that underwent different stages of functionalization ($n = 1$, 2 and 4). The results are shown in Fig. 3 from which one can immediately see that the change of the charge transfer resistance – *i.e.*, the difference of R_{ct} measured after and before the target is conveyed to the cell – is larger for $n = 1$ [Fig. 3(a)]. In fact, R_{ct} increases as n goes from 1 to 4 as a result of more Abs on the electrode, but this condition is not beneficial for the sensitivity.

With the same arguments used to define r_f, we can define the ratio r_s, which is due to the target recognition, as follows:

$$r_s = \frac{R_{ct\ C.\ Albicans} - R_{ct\ abs}}{R_{ct\ bare}}. \quad (2)$$

As we will see below, r_s has proven to be a robust and reliable biosensing parameter. The data in Fig. 3 provided for r_s the values 0.50, 0.35 and 0.33 for the number of the functionalization stages n being 1, 2, and 4, respectively. Considering that a too poor surface coverage could lead to issues with specificity, we deemed the surface functionalization achieved with $n = 1$ to be the optimal trade-off for achieving high sensitivity and specificity. It is important to note that the reason why an electrode only partially functionalized with Abs could be beneficial for the sensitivity without affecting the specificity (see below for the latter) lies in the large size of the target. Only few fungi can significantly cover part of the electrode and alter the charge transfer resistance.

Detection of *C. albicans* in GYP

A volume of 1 mL of GYP containing 10^6 cells was serially diluted in GYP to have samples (1 mL) with *C. albicans* in the range of 10^1–10^6 cells per mL. The samples flowed in the circuit for 1 hour at room temperature, allowing for the capture of *C. albicans* by the immobilized antibodies on the electrode surface. Subsequently, the electrode was rinsed with 0.01 M PBS for 15 minutes to remove any non-specifically or weakly bound *C. albicans* cells. The charge transfer resistance was then measured by dipping the electrode in the electrolytic solution.

The results are shown in Fig. S5† in which the errors arise from measurements carried out in duplicate or triplicate, whereas the experimental data were fitted by a logistic function. The shaded area represents the no-signal region when the 3SD criterion is adopted. In this case, the signal threshold is set above the control by 3 standard deviations. The relatively high uncertainty in the signal measured for the control can be attributed to fluctuations in the protein content of GYP, which is relatively high. It is evident that since the electrode surface was not fully covered, these proteins are capable of binding to the electrode in a non-specific manner. Nevertheless, even under these unfavorable conditions, a limit of detection of 10^2 CFU mL^{-1} can be safely deduced from Fig. S5.†

Detection of *C. albicans* in urine

In an effort to develop a biosensor for medical diagnostic applications, we tested our procedure for detecting *C. albicans*

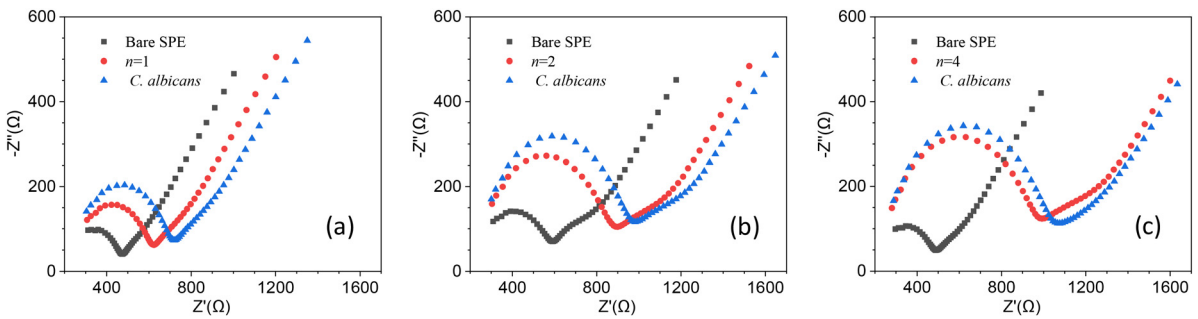

Fig. 3 EIS performed with three electrodes whose surfaces were functionalized with different degrees of surface coverage [(a) $n = 1$, low; (b) $n = 2$, moderate, and (c) $n = 4$ high, which corresponds to the electrode fully covered by Abs]. The target concentration was chosen to be 10^2 CFU mL^{-1} in order to optimize the biosensor response at low concentrations. By increasing the degree of the surface coverage, the charge resistance R_{ct} increases (red circles), but the change of resistance (ΔR_{ct}) – with respect to its value after the functionalization – is more visible with a low degree of surface coverage ($n = 1$).

in urine. We spiked an initial concentration of 10^7 CFU mL^{-1} of cells grown in GYP, and the dose–response curve is reported in Fig. 4. The experimental data resulted from measurements carried out in triplicate and were fitted by a logistic curve. All the measurements were performed by using different commercial gold screen printed electrodes, which are the main source of variability in this kind of biosensor as witnessed from the EIS spectra shown in Fig. 2. Thus, the tiny deviations of the experimental points from the logistic curve in Fig. 4 demonstrate the effectiveness of the normalization procedure described by eqn (1) and (2).

A comparison of the data obtained in urine with those measured in GYP (Fig. S5†) reveals a lower control value – as well as a lower uncertainty – in urine than in GYP. This significant difference has a notable influence on the limit of detection because, by applying the 3SD criterion (shaded area in Fig. 4), we can reach a value of 10 CFU mL^{-1}. As previously observed, this can be attributed to the high protein content in GYP. In fact, despite being a real sample, urine typically has a much lower concentration of analytes that could potentially interfere with the impedance measurement.

The presence of proteins in GYP can also explain the larger dynamic range exhibited by the detection of cells in urine. The dose–response curve suggests an asymptotic value for r_s of approximately 3, whereas in GYP, a saturation value of approximately 0.8 is observed. In fact, the presence of analytes (proteins) capable of binding to the partially covered electrode surface inherently reduces the effective area available for detection, thereby limiting the maximum detectable concentration.

Specificity test

To assess the specificity of the developed immunosensor for *C. albicans*, we conducted a test to evaluate the response of the functionalized immunosensor to another non-specific microorganism, *Escherichia coli*, which is known to cause a significant proportion of urinary tract infections.[37] Since *E. coli* can potentially be present in urine samples, it is a suitable candidate for the assessment of the lack of cross-reactivity. We carried out the test on different urine samples received in the laboratory for biochemical investigations and used as internal controls in bacteriology before being discarded.

An aliquot of urine of 1 mL was incubated with *E. coli* at a concentration of 10^6 CFU mL^{-1} and made to flow through the circuit for one hour at room temperature.

Subsequently, a washing step with PBS (0.01 M) was performed for 15 minutes to remove any non-specific bonds or contaminants. Fig. 5, which illustrates the changes in R_{ct}, demonstrates that the charge transfer resistance is only slightly higher than that of the negative control (1 mL of urine), whereas it is significantly lower than the value measured in *C. albicans* at the same concentration. This outcome was somewhat expected since we intentionally employed a surface that was not fully saturated with antibodies to enhance the visibility of the target microorganism. However, due to their smaller size, the bacteria may exhibit some interference. Nevertheless, in view of its application, we can confidently conclude that the specificity of the biosensor described here is more than satisfactory.

Test of the biosensor

To verify the reliability of our biosensor, we spiked *C. albicans* in 1.1 mL urine to have a concentration of 10^4 CFU mL^{-1}. Part of this volume (<100 μL) was used to yield four samples with different concentrations (10^4 CFU mL^{-1} and dilutions 1 : 10, 1 : 100, and 1 : 1000). A volume of 10 μL of each concentration was added to a Petri dish specifically designed for cultivating *C. albicans*, whereas the remaining part (≈1 mL) was used for biosensing measurements. Fig. 6 visually presents the presence and growth (24 hours) of fungal colonies at the spiked concentration and various dilutions. The colony count in the undiluted sample (10 μL) was ≈200 (197 colonies were actually recognized) and scaled with the dilutions accordingly. Thus the concentration measured by the cell growth method was 2×10^4 CFU mL^{-1}.

The measurement with the biosensor provided the value r_s = 0.75 ± 0.10 that corresponds (see Fig. 4) to a cell concentration

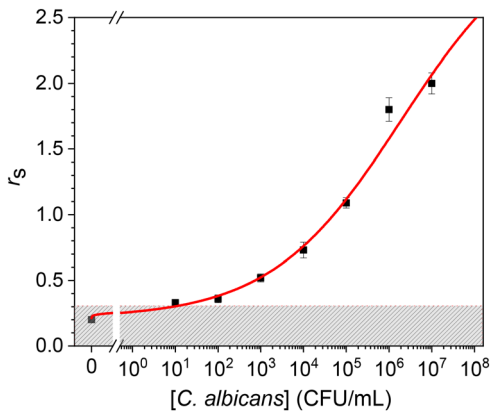

Fig. 4 Dose–response curve for the detection of *C. albicans* in urine.

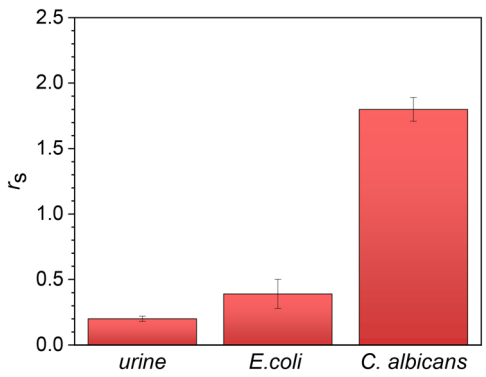

Fig. 5 Specificity test. At the same concentration of 10^6 CFU mL^{-1}, the signal from *C. albicans* is approximately four times larger than that from *E. coli*.

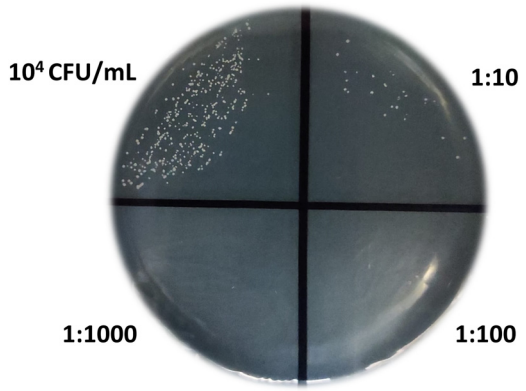

Fig. 6 This picture shows the growth of cells from the specimen at 10^4 CFU mL^{-1}. The initial specimen was diluted by three dilution factors, as shown in the figure. The four samples were then cultured on Petri dishes for 24 hours. The colony count in the undiluted sample was 197 which corresponds to 2×10^4 CFU mL^{-1}. The count scales accordingly with the dilution.

in the range 1–2 ($\times 10^4$) CFU mL^{-1}, which is in satisfactory agreement with the value achieved from the cell culture.

Conclusions

C. albicans is the most common cause of superficial and invasive fungal infections, and urine samples are obviously suitable for diagnosing urinary tract infections. The microbiological diagnosis of urinary infections is based on a cut-off that is generally set at 10^4–10^5 CFU mL^{-1}, although the detected concentration value is provided to a clinician for appropriate interpretation, even if it is lower than the cut-off. The need to have a good sensitivity at lower concentrations is especially critical in the case of newborns or suprapubic aspiration.[38] Moreover, diagnosing *Candida* infections typically relies on culture examination, which can take 48–72 hours for fungal isolation and identification. Therefore, there is a strong need for a rapid and reliable test to detect this infection. To meet this demand, we have developed an electrochemical impedance immunosensor that utilizes commercial screen-printed electrodes for the fast and sensitive detection of *C. albicans* in urine.

The gold surface of the electrode was functionalized with antibodies using a UV-activation technique known as the Photochemical Immobilization Technique (PIT)[34] – a procedure recently recognized for its remarkable effectiveness in tethering Abs to gold surfaces.[39] The change in charge transfer resistance (R_{ct}) served as the indicator of the presence of *C. albicans*.

Interestingly, we found that for targets as large as fungi, partial coverage of the surface resulted in a stronger signal that allowed us to achieve a limit of detection of 10 CFU mL^{-1} in urine. While this limit can generally be reached or exceeded (at least in simple matrices), it is noteworthy that our biosensor utilizes commercial screen-printed electrodes, which we incorporated into a fluidic design to optimize the interaction between the target and the surface. As a result, we were able to measure the concentration of *C. albicans* in urine in less than 90 minutes with a procedure that is virtually independent of the operator.

Given the simplicity of the equipment required to carry out the measurements, our biosensor lends itself as a point-of-care device. Moreover, both the cell and the fluidic components can be easily upgraded to create a multiplexing device. Overall, the combination of microfluidics and electrochemical impedance spectroscopy described here offers significant advantages only in terms of improved sensitivity, enhanced throughput, and precise control of fluidic parameters.

Author contributions

Tina D'Aponte: investigation, data curation and writing – original draft. Maria De Luca: data curation and software. Nikola Sakač: formal analysis and writing – original draft. Martina Schibeci: resources and validation. Angela Arciello: resources and writing – review & editing. Emanuela Roscetto: resources and validation. Maria Rosaria Catania: resources and validation. Vincenzo Iannotti: methodology and writing – review & editing. Raffaele Velotta: methodology, formal analysis, writing – review & editing and supervision. Bartolomeo Della Ventura: conceptualization, methodology, data analysis, funding acquisition, and writing – review & editing.

Conflicts of interest

"There are no conflicts to declare".

Acknowledgements

This study was carried out within the Agritech National Research Center and received funding from the European Union Next-GenerationEU (PIANO NAZIONALE DI RIPRESA E RESILIENZA (PNRR) – MISSIONE 4 COMPONENTE 2, INVESTIMENTO 1.4 – D.D. 1032 17/06/2022, CN00000022).

References

1 J. F. Fisher, *Clin. Infect. Dis.*, 2011, **52**, S429–S432.
2 W. A. Alfouzan and R. Dhar, *J. Mycol. Med.*, 2017, **27**, 293–302.
3 P. Datta, M. Kaur, S. Gombar and J. Chander, *Indian J. Crit. Care Med.*, 2018, **22**, 56–57.
4 M. Gajdács, I. Dóczi, M. Ábrók, A. Lázár and K. Burián, *Cent. Eur. J. Urol.*, 2019, **72**, 209–214.
5 T. T. Özer, S. Durmaz and E. Yula, *J. Infect. Chemother.*, 2016, **22**, 629–632.
6 P. Behzadi, E. Behzadi and R. Ranjbar, *Cent. Eur. J. Urol.*, 2015, **68**, 96–101.
7 L. Toner, N. Papa, S. H. Aliyu, H. Dev, N. Lawrentschuk and S. Al-Hayek, *QJM*, 2016, **109**, 325–329.
8 E. E. Nejad, P. G. N. Almani, M. A. Mohammadi and S. Salari, *J. Clin. Lab. Anal.*, 2020, **34**, 1–8.

9 P. L. White, J. S. Price, A. Cordey and M. Backx, *Curr. Fungal Infect. Rep.*, 2021, **15**, 67–80.
10 E. K. Dennis, S. Chaturvedi and V. Chaturvedi, *Front. Microbiol.*, 2021, **12**, 757835.
11 K. Wang, Y. Luo, W. Zhang, S. Xie, P. Yan, Y. Liu, Y. Li, X. Ma, K. Xiao, H. Fu, J. Cai and L. Xie, *Mycoses*, 2020, **63**, 181–188.
12 C. Rizzato, L. Lombardi, M. Zoppo, A. Lupetti and A. Tavanti, *J. Fungi*, 2015, **1**, 367–383.
13 E. Svetličić, L. Dončević, L. Ozdanovac, A. Janeš, T. Tustonić, A. Štajduhar, A. L. Brkić, M. Čeprnja and M. Cindrić, *Molecules*, 2022, **2717**, 54–61.
14 K. K. Hussain, D. Malavia, E. M. Johnson, J. Littlechild, C. P. Winlove, F. Vollmer and N. A. R. Gow, *J. Fungi*, 2020, **6**, 1–26.
15 L. Mendive-Tapia, D. Mendive-Tapia, C. Zhao, D. Gordon, S. Benson, M. J. Bromley, W. Wang, J. Wu, A. Kopp, L. Ackermann and M. Vendrell, *Angew. Chem.*, 2022, **61**, e202117218.
16 D. Yu, L. Wang, H. Zhou, X. Zhang, L. Wang and N. Qiao, *Bioconjugate Chem.*, 2019, **30**, 966–973.
17 Y. Zhang, H. Duan, Y. Liu, Y. Li and J. Lin, *Comput. Electron. Agric.*, 2023, **206**, 107702.
18 E. Cesewski and B. N. Johnson, *Biosens. Bioelectron.*, 2020, **159**, 112214.
19 M. Sarabaegi and M. Roushani, *Anal. Methods*, 2019, **11**, 5591–5597.
20 J. Wu, H. Liu, W. Chen, B. Ma and H. Ju, *Nat. Rev. Bioeng.*, 2023, **1**, 1–15.
21 L. De Brito Ayres, J. Brooks, K. Whitehead and C. D. Garcia, *Anal. Chem.*, 2022, **94**, 16847–16854.
22 P. Dutta, Y. J. Lu, H. Y. Hsieh, T. Y. Lee, Y. T. Lee, C. M. Cheng and Y. J. Fan, *Micromachines*, 2021, **12**, 166.
23 S. Tvorynska, J. Barek and B. Josypčuk, *Sens. Actuators, B*, 2021, **13**, 2–52.
24 M. Cimafonte, A. Fulgione, R. Gaglione, M. Papaianni, R. Capparelli, A. Arciello, S. B. Censi, G. Borriello, R. Velotta and B. Della Ventura, *Sensors*, 2020, **20**, 274.
25 C. Zhang, Y. Su, S. Hu, K. Jin, Y. Jie, W. Li, A. Nathan and H. Ma, *ACS Omega*, 2020, **5**, 5098–5104.
26 D. Kwasny, S. E. Tehrani, C. Almeida, I. Schjødt, M. Dimaki and W. E. Svendsen, *Sensors*, 2018, **18**, 1–9.
27 A. G. da Silva-Junio, I. A. M. Frias, R. G. Lima-Neto, L. Migliolo, P. S. e Silva, M. D. L. Oliveira and C. A. S. Andrade, *J. Pharm. Biomed. Anal.*, 2022, **216**, 114788.
28 K. L. Ribeiro, I. A. M. Frías, A. G. Silva, R. G. Lima-Neto, S. R. Sá, O. L. Franco, M. D. L. Oliveira and C. A. S. Andrade, *Biochem. Eng. J.*, 2021, **167**, 107918.
29 S. R. Sá, A. G. Silva Jr, R. G. Lima-Neto, C. A. S. Andrade and M. D. L. Oliveira, *Talanta*, 2020, **220**, 121375.
30 R. D. Crapnell, A. Garcia-Miranda Ferrari, N. C. Dempsey and C. E. Banks, *Sens. Diagn.*, 2022, **1**, 405–428.
31 J. L. de Miranda, M. D. L. Oliveira, I. S. Oliveira, I. A. M. Frias, O. L. Franco and C. A. S. Andrade, *Biochem. Eng. J.*, 2017, **124**, 108–114.
32 L. A. Layqah and S. Eissa, *Microchim. Acta*, 2019, **186**, 224.
33 L. M. Fischer, M. Tenje, A. R. Heiskanen, N. Masuda, J. Castillo, A. Bentien, J. Émneus, M. H. Jakobsen and A. Boisen, *Microelectron. Eng.*, 2009, **86**, 1282–1285.
34 B. Della Ventura, M. Banchelli, R. Funari, A. Illiano, M. De Angelis, P. Taroni, A. Amoresano, P. Matteini and R. Velotta, *Analyst*, 2019, **144**, 6871–6880.
35 R. Funari, B. Della Ventura, C. Altucci, A. Offenhäusser, D. Mayer and R. Velotta, *Langmuir*, 2016, **32**, 8084–8091.
36 T. Bertok, L. Lorencova, E. Chocholova, E. Jane, A. Vikartovska, P. Kasak and J. Tkac, *ChemElectroChem*, 2019, **6**, 989–1003.
37 R. D. Klein and S. J. Hultgren, *Nat. Rev. Microbiol.*, 2020, **18**, 211–226.
38 M. G. Coulthard, *Pediatr. Nephrol.*, 2019, **34**, 1639–1649.
39 M. Conrad, G. Proll, E. Builes-Münden, A. Dietzel, S. Wagner and G. Gauglitz, *Microchim. Acta*, 2023, **190**, 62.